



## **OPENFOAM APPLICATION ON PERFORMANCE PREDICTIONS OF AN INDUSTRIAL CENTRIFUGAL FAN WITH AIRFOIL BLADES**

Jing WANG and Marcel KAMUTZKI

*DALTEC PROCESS FANS, 465 Laird Rd. Guelph,  
Ontario N1G 4W1 Canada*

### **SUMMARY**

This paper presents a modelling approach using OpenFOAM of an airfoil bladed centrifugal fan which was developed for performance predictions of our regular industrial products. The hexahedral dominant mesh was generated with boundary layers on the fan wall surfaces. The frozen rotor approach was employed for predicting the flow field of the entire impeller in an asymmetric housing. The k-epsilon model and k-omega Shear Stress Transport (SST) model were used for the turbulence for a comparison purpose. The customized template for the performance predictions is described. The results of dimensionless pressure and power using the two turbulence models are discussed and future development on the CFD model is recommended.

### **INTRODUCTION**

Performance prediction of industrial centrifugal fans is always an interesting and challenging topic for industrial fan designers. CFD packages are more widely applied to achieve such a purpose as hardware costs are reduced. Although commercial CFD codes can provide strong meshing tools and mature CFD solvers for fan performance predictions, some diligent engineers are more interested in using open-source codes, such as OpenFoam, for their fan simulations because there are no limitations on parallel computations. In addition, the customizable and scriptable templates can be easily used to parameterize the numerical calculations.

In practice, an industrial fan operates under variable conditions of air supply, covering an enormous range of the performance curve. The approximate performance of a fan is usually determined by introducing correction terms and estimation of losses calculated from available semi-empirical equations, or using fan laws based on selected test data. These approaches have provided excellent results in the optimum near-design conditions, with reduced accuracy farther from the design point. New fan design is difficult to establish without first building a scale model and performing physical testing. Relatively speaking then, the CFD method can provide better computational fidelity if a proper model is developed. The model can further evolve into a superior tool for design and optimization of industrial fan and thus can reduce the R&D expenses of a new product. A. Corsini,

et al. investigated aerodynamic characteristics of a high-pressure centrifugal fan using OpenFoam and developed a steady state model for incompressible flow using a standard k-epsilon turbulence model and 6.7 million structured mesh cells [1]. L. Cardino, et al. further applied the CFD model to predict the performance of an industrial centrifugal fan incorporating cambered plate impeller blades and compared the numerical results with the test data in a reasonable degree of accuracy (~3%) [2]. On the other hand, the problem of fan energy consumption is found to be significant for many international regulations. Nowadays, all fan manufacturers are being charged with a duty to produce equipment meeting very high requirements of energy efficiency and performance such as those detailed in the Commission Regulation (No. 327/2011) of the European Union [3]. While it is currently not clear what form it will take, energy efficiency regulations are being developed in the United States as well. Therefore, to develop a reliable and innovative prediction tool for the performance of an industrial fan is not only the interest of fan designers but it is also becoming a requirement of our communities.

This paper presents an effort on an OpenFoam application of an airfoil bladed centrifugal fan which we developed for performance predictions of our regular industrial products. In the CFD model, the snappyHexMesh utility was applied to create the hexahedral dominant mesh with boundary layers on the wall surfaces. The multiple reference frame (MRF) model was employed for the simulation of rotation zone. The k-epsilon model [4] and k-omega Shear Stress Transport (SST) model [5] were used for the turbulence flow in the fan model. A customized template for the fan performance predictions, as well as the parallel computation setup and postprocessing, are also described in the paper. The results of dimensionless pressure and power using the two turbulence models are compared and the corresponding pressure and velocity fields of the centrifugal fan are discussed. Finally, the future development on the CFD model is recommended.

## NUMERICAL APPROACH

### Centrifugal fan description

The centrifugal fan under investigation was selected from the airfoil blade series of our regular industrial products for engineering applications. Figure 1 illustrates the fan geometry, which consists of three parts: the inlet cone, the impeller and the casing and outlet duct system. Table 1 lists the technical specifications of the centrifugal fan.

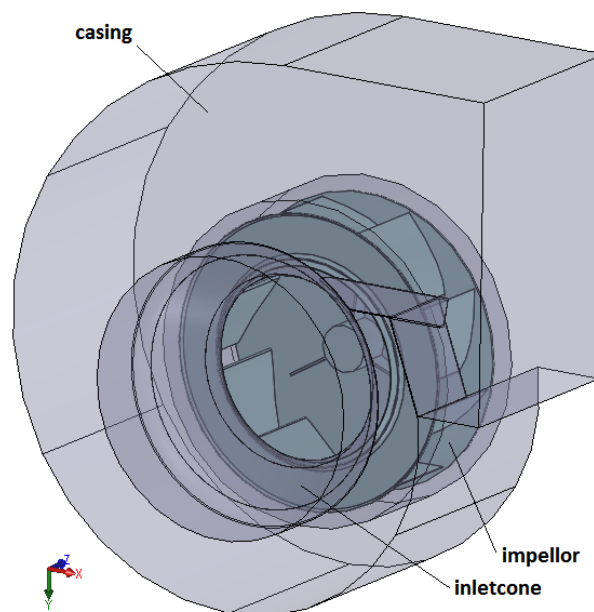


Figure 1: The centrifugal fan under investigation

The snappyHexMesh utility was used to generate a 3D mesh containing hexahedra (hex) and split-hexahedra (split-hex) automatically from the centrifugal fan geometry in Stereolithography (STL) format. The meshing utility first refined a background mesh and then refined the resulting mesh to the fan geometry surfaces. Boundary layers were inserted on the wall surfaces thereafter. Figure 2 shows the snappyHexMesh for the centrifugal fan with 5 boundary layers on the wall surfaces. The total number of the computational grid elements is  $10.9 \times 10^6$  and the relative final layer thickness is set to 0.64.

Table 1: Essential dimensions of the centrifugal fan

Inlet blade width	$b_1 = 0.272 \text{ m}$
Outlet blade width	$b_2 = 0.272 \text{ m}$
Inlet blade angle	$\beta_1 = 14^\circ$
Outlet blade angle	$\beta_2 = 32^\circ$
Width of fan casing	$W_b = 0.622 \text{ m}$
Impellor nominal diameter	$D_{imp} = 0.838 \text{ m}$
Seal ring diameter	$d_i = 0.596 \text{ m}$
Blade number	$N = 9$
Rotational speed	$\omega = 1500 \text{ rpm or } 25 \text{ Hz}$

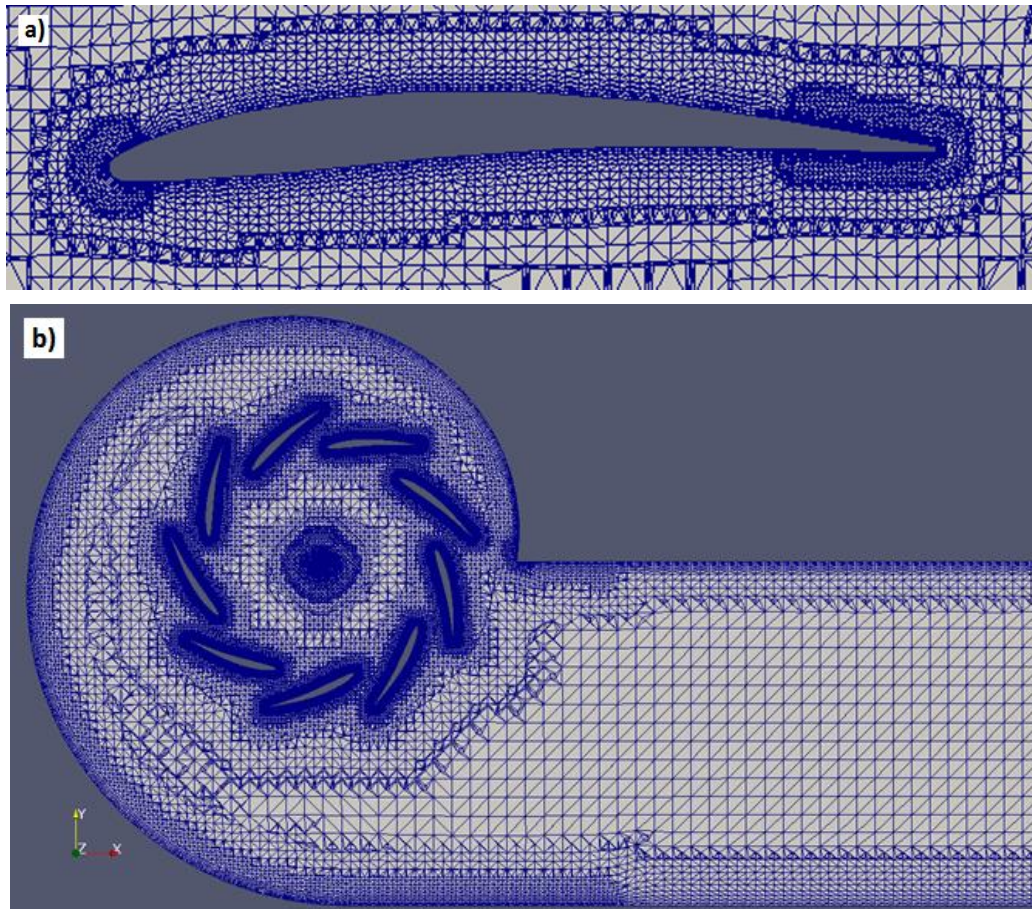


Figure 2: Computational snappyHexMesh for the centrifugal fan:  
(a) blade mesh with 5 boundary layers, (b) impeller and casing interface

The predictions are expressed in terms of dimensionless inlet volume flow coefficient ( $\varphi$ ), fan total pressure coefficient ( $\psi$ ) and impeller power coefficient ( $\lambda$ ) [1] which are defined as followings:

$$\varphi = \frac{4Q}{\pi^2 \omega D_{imp}^3} \quad (1)$$

$$\psi = \frac{2\Delta p_t}{\pi^2 \rho \omega^2 D_{imp}^2} \quad (2)$$

$$\lambda = \frac{8P}{\pi^4 \rho \omega^3 D_{imp}^5} \quad (3)$$

where  $D_{imp}$  is the impeller nominal diameter, m;  $\omega$  is rotational speed, Hz;  $\rho$  is the inlet air density, kg/m<sup>3</sup>;  $\Delta p_t$  is the fan total pressure rise, Pa;  $P$  is the impeller power, W; and  $Q$  is the inlet volume flow rate, m<sup>3</sup>/s.

### Computational method

The numerical approach was developed using the opensource CFD code OpenFoam-dev [6]. The incompressible Reynold-Averaged Navier-Stokes equations were solved using the finite volume method. The turbulence was modelled using the k-epsilon model and k-omega Shear Stress Transport (SST) model respectively. Corresponding wall functions are applied to close the turbulence equations.

The entire centrifugal fan was modelled due to the asymmetric structure of casing. The multiple reference frame (MRF) model was employed for the simulation of a rotating zone, which enables the Coriolis and centrifugal body forces within the impeller to be accounted for.

Simulations were conducted using the simpleFoam solver with the UPWIND divergence scheme, a GAMG linear solver for the pressure field and smoothSolver for all other computed quantities. Eight cores of Intel Xeon E5-2667v3 3.2G were used for the parallel computation in an Ubuntu system.

### Airfoil bladed fan template

Fan geometry was created using Solidworks. Each part of the fan model was exported in a format of surface (and/or solid) STL file and all the exported STL files were manually assembled to one STL file. Then, the template was used to read the assembled STL file and create a corresponding snappyhexmesh with boundary layers (if required).

Figure 3 shows the file structure of the airfoil fan template. The emesh files created by the executable snappyHexMesh utility are stored in folder “constant”. The meshing control is defined in the “snappyHexMeshDict” file in folder “system”. A Multiple Reference Frame (MRF) approach is applied for fan modelling, which is defined in the “MRFProperties” file in folder “constant”. The fan speed is 1500rpm (or 157.08 rad/s). Folder “0” includes the files for initial and boundary conditions, such as p for the pressure scalar fields at boundaries, “U” for the velocity vector fields, “k, nut and omega” for turbulence fields of k-omega SST model. Inlet and outlet boundary conditions are also defined in folder “0”. For instance, the outlet boundary is set as a mass flow rate with a magnitude and the inlet p is defined as zero total pressure. Discretization schemes, solver and Finite Volume method (FVM) selections, and relaxation factor setup can be defined in the files of “fvSchem” and “fvSolution” of folder “system”. The “decomposeParDict” file in folder “system” is setup for parallel computation control. The hierarchical method with eight CPU cores is currently applied for the simulation. The outlet static pressure and impeller moments are monitored for postprocessing, which are defined in the “controlDict” file of folder “system”.



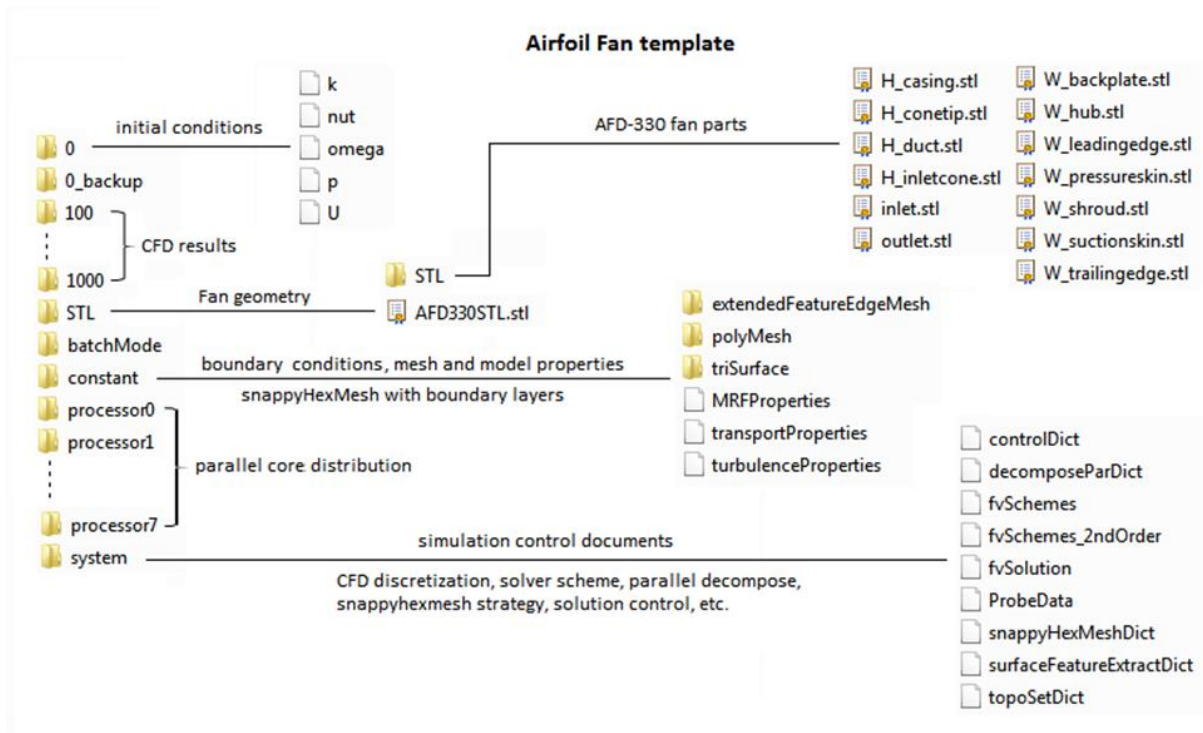


Figure 3: Structure of airfoil fan template

### Grid sensitivity analysis

Simulation sensitivity to grid density was studied. The power coefficient and total pressure coefficient are identified as convergence parameters, Table 2. An initial coarse mesh with 8 million cells was compared to the final fine mesh with 11 million cells. Dimensionless wall distance ( $y^+$ ) values onto solid walls are also included.

Table 2: Grid sensitivity analysis and  $y^+$  on solid surfaces

	Coarse	Fine	
Power coefficient	0.213	0.218	
Total pressure coefficient	0.825	0.840	
$y^+$ on solid surfaces			
	Min.	Max.	Avg.
Blade pressure	0.08	153.93	28.19
Blade suction	0.08	251.42	36.75
Shroud	0.13	175.44	21.35
Hub	1.53	421.76	50.24
Casing	0.01	1319.74	36.18

## RESULTS AND DISCUSSION

### Dimensionless performance curves

Figure 5a shows the relationship of inlet volume flow coefficient and fan total pressure coefficient. Figure 5b is the curve of the impellor power coefficient. For the  $k$ - $\omega$  SST model, the maximum pressure coefficient is 0.840 at the volume flow coefficient of 0.094, while the maximum power

coefficient is 0.231 at the volume flow coefficient equal to 0.129. The k-epsilon model predicts lower pressure and higher power than the k-omega SST model does. There is approximately 3~4% difference between the two sets of curves.

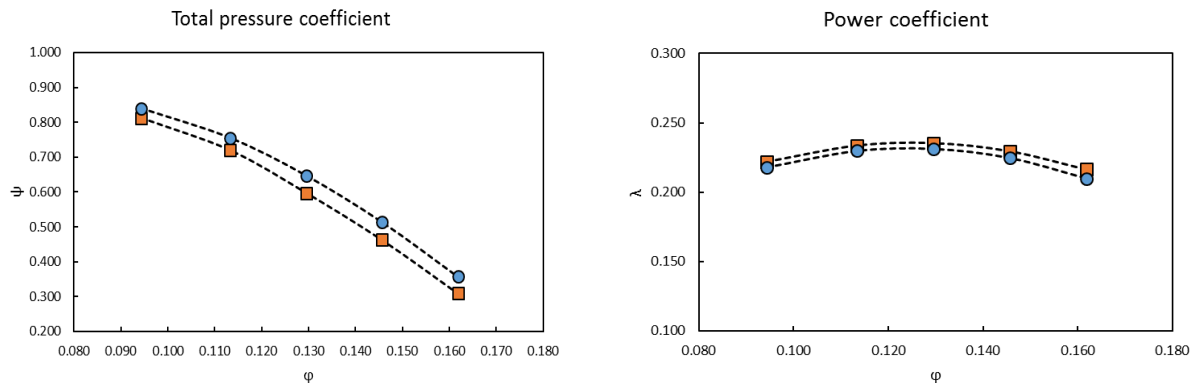


Figure 5: Fan dimensionless performance curve  
 (symbols: circle in blue --- k-omega SST, square in brown --- k-epsilon)

### Pressure and velocity fields

Figure 6 shows the pressure distributions in the cross-section of the impeller (at 50% of blade width) for the selected three operating points covering the entire calculating range of fan curves. The upper three plots are predicted by the k-epsilon model, while the lower ones are done by the k-omega SST model.

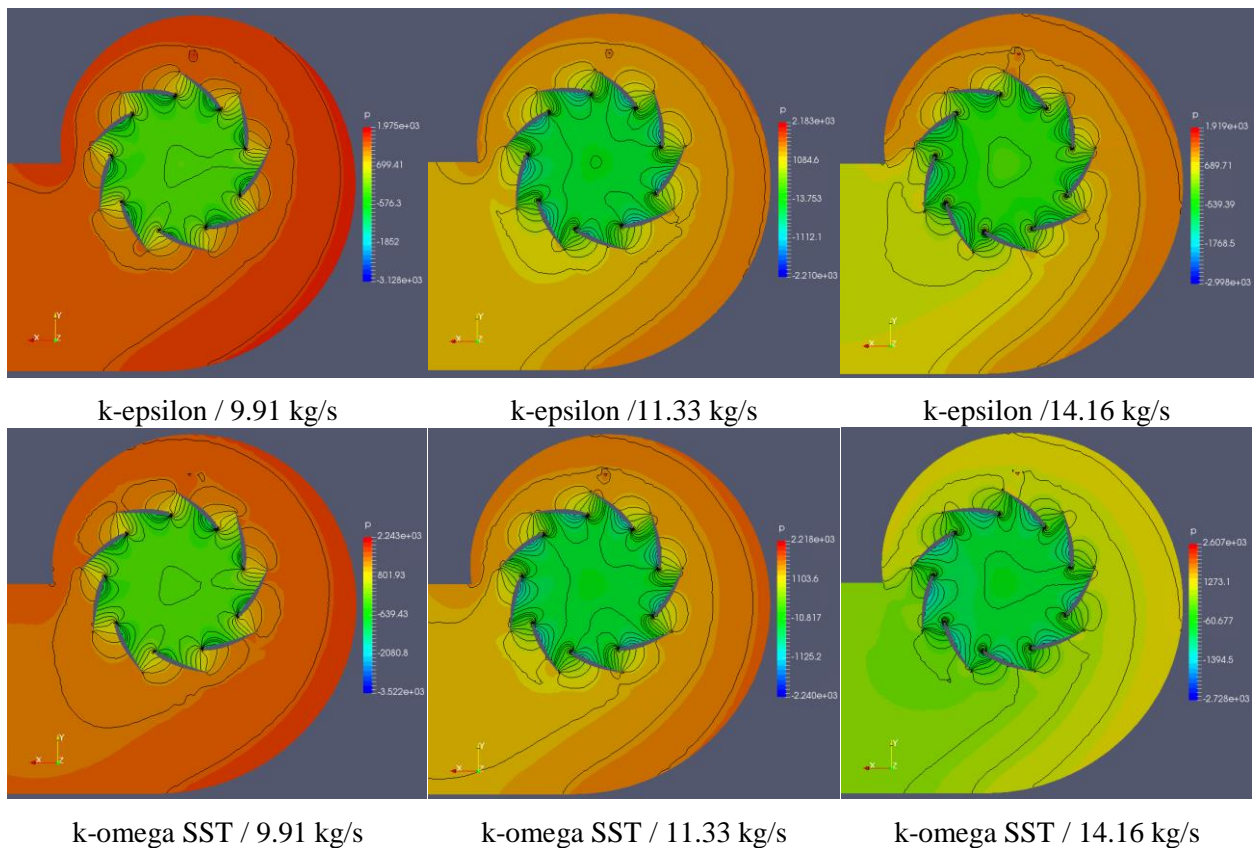


Figure 6: Pressure contours of impellor channels

Figure 7 illustrates the scalar velocity contours at the same cross-section of the impellor. The velocity distributions around the blades predicted by the two turbulence models are observed to be almost identical. The difference between the results of the two models is on the pressure



predictions, indicating the normal force on the blade surface is the major cause of the deviations on the dimensionless pressure and power curves.

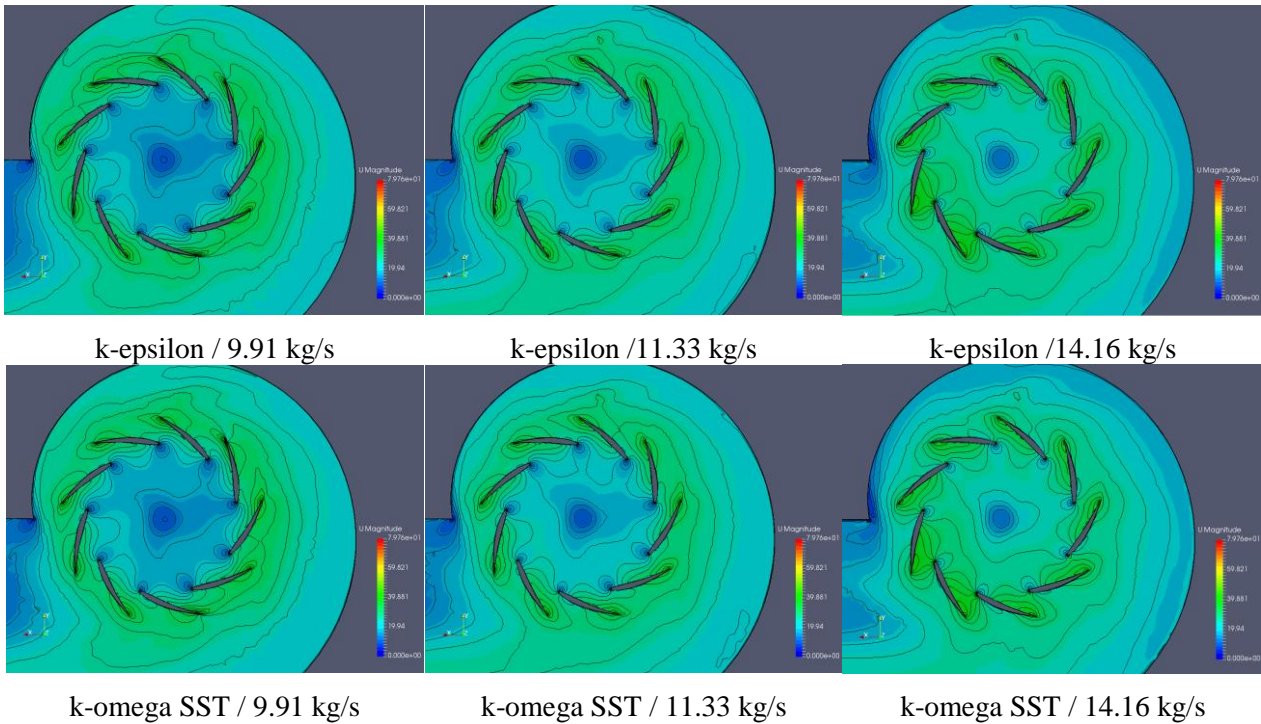


Figure 7: Velocity contours of impeller channels

Figure 8 shows the surface flow of Line Integral Convolution (LIC) on the y-z plane at x equal to zero. The complex flow goes from the inlet cone, through the impeller and finally into the casing. The main flow orientation is observed to be changed in 90 degrees, due to the wheel rotation around the z-axis. The flow in the inlet region is well organized, while strong vortices are observed near the impeller backplate and shroud edges as the flow is exiting the impeller.

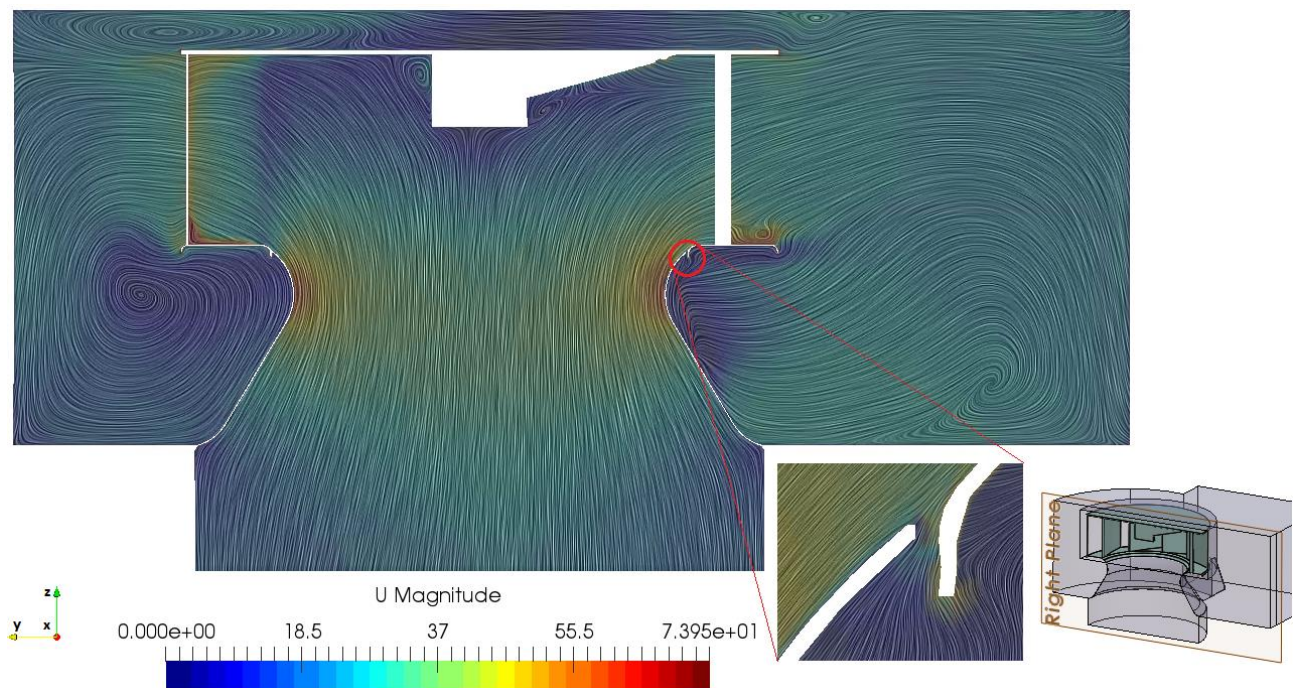


Figure 8: Surface oilflow of inlet cone, impeller and casing channels  
 (*k-omega SST*, mass flow rate is 11.33kg/s)

## CONCLUSIONS AND RECOMMENDATIONS

In the present study, an airfoil bladed centrifugal fan selected from our regular products was modelled using OpenFoam. The CFD tool was developed for assessing the complete flow characteristics and performance of the centrifugal fan to overcome the shortcomings of using empirical or similarity approaches;

Based on the developed numerical model, a robust convergence of CFD solutions to the characteristics of the rotating machine was observed. The primary indicators of the fan, i.e. pressure rise and power consumption were obtained from the simulation. Additionally, the flow structure inside the impeller and casing channels, such as vortices in the casing and hub areas, flow separations at the casing tongue or cutoff, etc. was illustrated.

For the future work, an experimental study has been planned to validate the numerical predictions by the CFD model. Some efforts in the aspects of numerical fidelity and operation automation are recommended. In addition, optimization on the fan performance using the CFD model is also expected.

## BIBLIOGRAPHY

- [1] A. Corsini, G. Delibra, et al. – *Aerodynamic Simulation of a High-pressure Centrifugal Fan for Process Industries*, GT2013-94982, Proceedings of ASME Turbo Expo 2013: Turbine Technical Conference and Exposition, **2013**
- [2] L. Cardillo, A. Corsini, et al., – *Predicting the Performance of an Industrial Centrifugal Fan Incorporating Cambered Plate Impellor Blades*, Chapter 11, The Application of Computational Methods in Industrial Fan Design, edited by Geoff Sheard, **2016**
- [3] COMMISSION REGULATION (EU) No. 327/2011,  
<http://eur-lex.europa.eu/legal-content/EN/TXT/?uri=CELEX%3A32011R0327>, **2017**
- [4] B.E. Launder, D.B. Spalding, – *The numerical computation of turbulent flows*, Computer Methods in Applied Mechanics and Engineering. 3 (2): 269–289. doi:10.1016/0045-7825(74)90029-2, **1974**
- [5] F. R. Menter – *Two-Equation Eddy-Viscosity Turbulence Models for Engineering Applications*, AIAA Journal, 32, (8), 1598, **1994**
- [6] OpenFoam download website, <https://openfoam.org/version/dev/>, **2017**